CHAPTER 3: LINEARLY TAPERED MEANDER LINE CROSS DIPOLE CIRCULARLY POLARIZED ANTENNA FOR UHF RFID TAG APPLICATIONS

3.1 Introduction

In all practical applications, passive RFID system with a larger read range is requisite. The read range, which is defined as the maximum distance at which a reader can detect the tag, can be enhanced by using greatly sensitive signal detection tag ICs, the use of which however increases the cost of the RFID systems. Read range can be augmented by increasing the radiated power from the RFID reader. However, the regulatory authorities of individual countries regulate the maximum radiated power in terms of Effective Isotropic Radiated Power (EIRP) [10]. Read range can also be enlarged by removing the polarization mismatch between the reader and the tag antennas. Since most UHF RFID systems employ Linearly Polarized (LP) tag antenna [160], Circularly Polarized (CP) antenna is used for reader applications to increase the reliability of detection of arbitrarily oriented tag antenna [161]. Due to the polarization mismatch, only half of the transmitted power from the CP reader antenna is received by the LP tag antenna. The polarization efficiency can be increased by using circularly polarized tag antenna instead of linearly polarized tag antenna. Apparently, the maximum read range of an RFID system with CP tag antenna can be improved by 41 % compared to the LP tag antenna due to 3 dB increase in power received by the CP tag antenna.

In this chapter, a meandered cross dipole tag antenna design with circularly polarized radiation in UHF band is presented. The antenna has a planar geometry with compact size and the conjugate matching of the complex input impedance between the antenna and the tag IC is realized by using a T-match network. The proposed antenna is comprised of two unequal length orthogonal dipoles with each arm of the dipoles consisting of a linearly tapered meander line and rectangular-shaped tip loading for size miniaturization [162]. Two semi-circular curves are inserted between the arms of one of the dipoles for CP radiation. The appropriate phase and magnitude relationship to obtain the circularly polarized radiation is achieved by properly choosing the length of the orthogonal dipoles.

3.2 Antenna Design

Geometry of the proposed linearly tapered meander line cross dipole antenna with circular polarization is shown in figure 3.1. Optimized geometrical parameters of the proposed antenna are exhibited in table 3.1. The antenna is designed for passive UHF RFID tag applications and is built on an FR4 glass epoxy substrate (ε_r=4.4 and tan δ=0.02) of thickness 1.6 mm. The intermediate stages of the evolution of the designed antenna structure are shown in figure 3.2.

The first design step is a dipole antenna. Dipole antennas are popular among various tag antennas due to their simple structure, omnidirectional radiation pattern and easier control of input impedance. But the length of any linear dipole antenna at UHF band is 16.4 cm which is larger than the standard label dimensions. Miniaturization of antenna size is done by using meandering technique to fit the antenna within the standard label dimensions. Meander line Dipole Antenna (MDA) resonates at a lower frequency in comparison to Linear Dipole Antenna (LDA) of same length [17]. Meander line structure helps in reducing the size of the antenna.

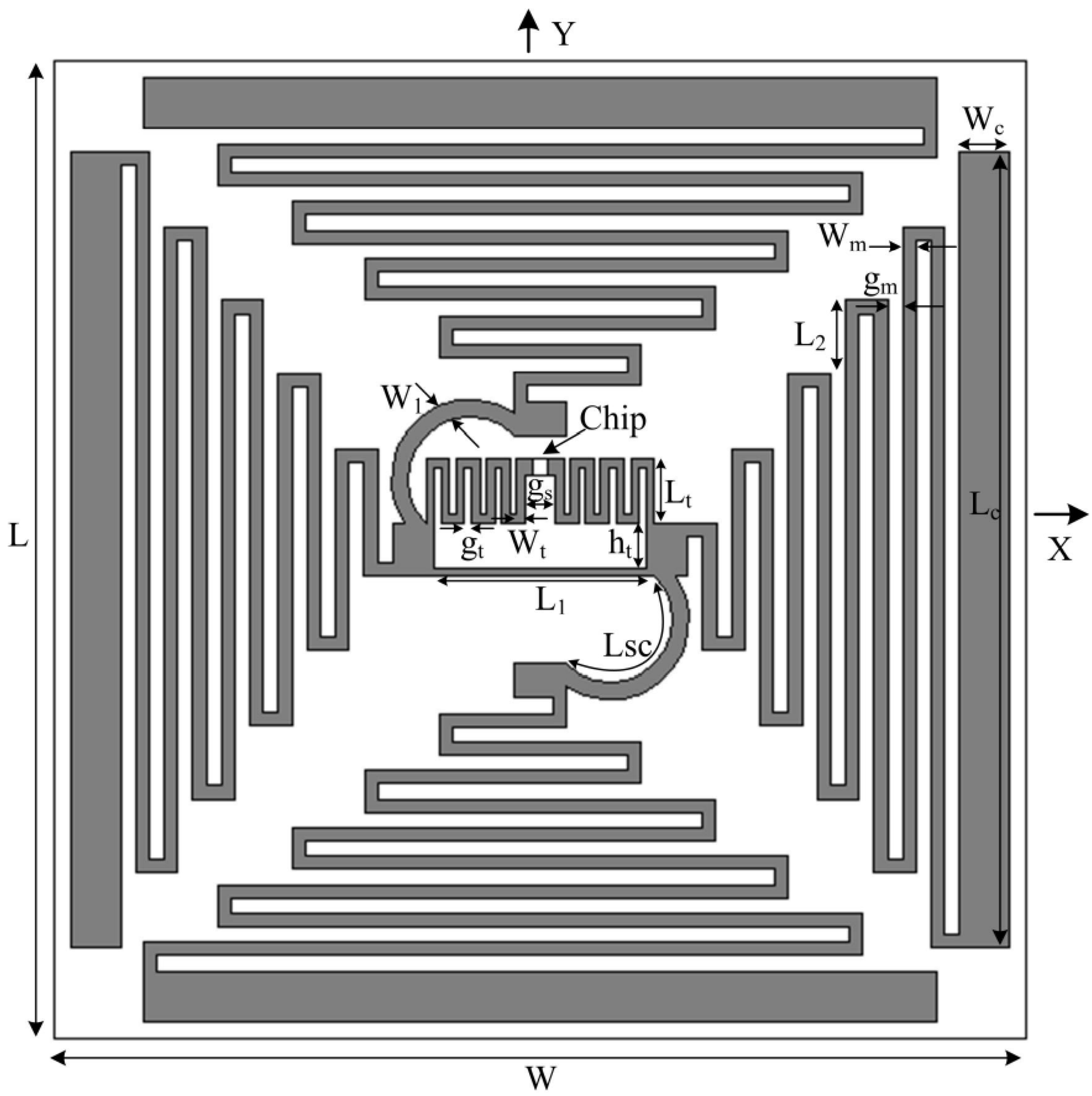

Figure 3.1 Geometry of the linearly tapered meander line cross dipole CP antenna

Table 3.1 Optimized geometrical parameters of the cross dipole CP antenna

Parameter	Value (mm)	Parameter	Value (mm)
L	58	$\mathbf{W_1}$	1
W	58	$\mathbf{W_m}$	0.8
$\mathbf{L_c}$	47.2	$\mathbf{g_m}$	0.9
$\mathbf{W_c}$	3	$\mathbf{L_t}$	3.8
$\mathbf{W_t}$	0.5	$\mathbf{h_t}$	3.2
$\mathbf{g_t}$	0.4	$\mathbf{g_s}$	1.8
$\mathbf{L_1}$	12.6	$\mathbf{L_2}$	4.4
Lsc	11.5		

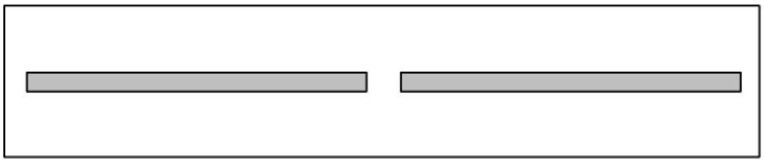

(a)

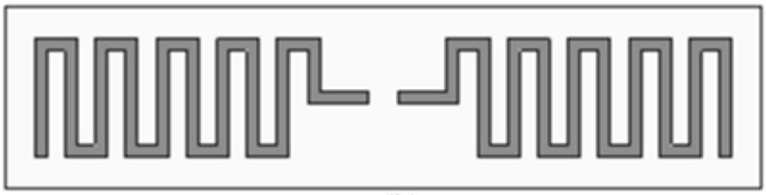

(b)

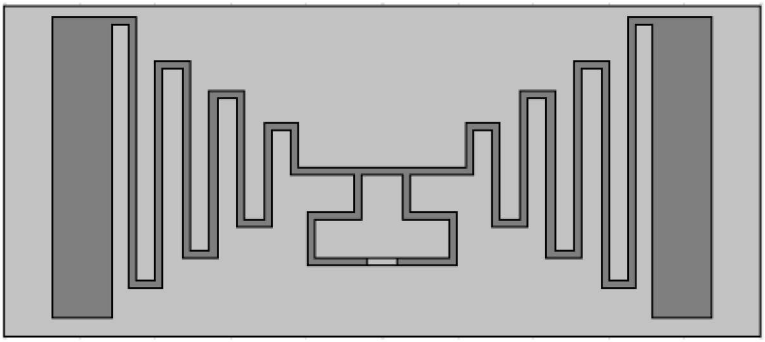

(c)

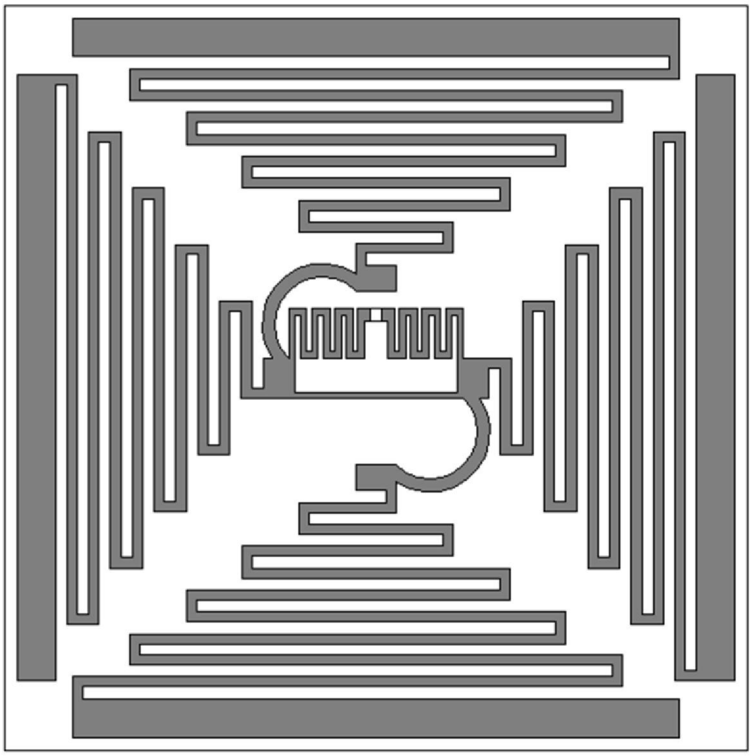

(d)

Figure 3.2 Intermediate stages of the evolution of the designed antenna structure, (a) Linear dipole, (b) Meander line antenna, (c) Linearly tapered meander line antenna, and (d) Cross dipole CP antenna

In case of uniformly meandered antenna, the overall efficiency is reduced due to the equal size of adjacent vertical elements carrying opposite current, effectively cancelling each other's radiation. Thus, in a uniform meander line antenna, radiation takes place only from the unidirectional current carrying horizontal elements with low efficiency. Therefore, in figure 3.2 (c), tapered meander line is used instead of uniform meandering in order to improve efficiency. In meander line antenna, current amplitude is the maximum in the centre and most of the charge storage takes place at the two ends where two rectangular strips are in place of sufficient surface area. The two obvious advantages of tip loading are reduction of the size and decrease in the capacitive reactance of the antenna, which helps in impedance matching with the capacitive chip. At the centre, a T-match network is used to provide inductive reactance to the antenna.

In figure 3.2 (d), the proposed CP antenna is shown, which comprises two cross dipoles. The vertical dipole is located at the neutral potential plane of the horizontal dipole to mitigate the coupling effect between two dipoles. Each arm of the orthogonal dipoles consists of a linearly tapered meander line and a rectangular shaped tip loading at the end. These two approaches, viz., meander line and capacitive tip loading, are adopted with dipoles to provide compactness in the size of the antenna. However, the antenna characteristics, such as efficiency and impedance bandwidth are degraded with the compactness in size.

3.3 Generation of Circularly Polarised Radiation

To generate circularly polarized radiation, two orthogonal dipoles excited with equivalent magnitude and out of phase are requisite [163]. The two orthogonal dipoles can be excited in parallel by using a single feed network [164] and the needed phase relationship for CP radiation is attained by using unequal length dipoles. Two semi-circular curves are connected with vertical dipole to get the appropriate phase relationship. By properly adjusting the length of the semi-circular curves, the electrical length of vertical dipole becomes slightly longer than half wavelength and the electrical length of the horizontal dipole becomes slightly shorter at the resonant frequency. Thus, at the desired resonant frequency (915 MHz) the longer (vertical) dipole has an inductive reactance, and the shorter (horizontal) dipole has a capacitive reactance [165]. The input impedance of horizontal (short) dipole is Z_a=22.05+j136.8 Ω at 915 MHz. By using chip impedance Z_c=11-j143 Ω at 915 MHz, the reflection coefficient and phase is calculated as follows:

$$\Gamma = \frac{Z_a - Z_c^*}{Z_a + Z_c} \tag{3.1}$$

$$= \frac{(22.05 + j136.8) - (11 + j143)}{(22.05 + j136.8) + (11 - j143)} = 0.376\angle -18.67^0$$

For the horizontal dipole, the phase angle of reflection coefficient is -18.67^0. The input impedance of long (vertical) dipole is Z_a=12.03+j149.41 Ω at 915 MHz. The reflection coefficient and phase corresponding to longer dipole is calculated as follows:

$$\Gamma = \frac{(12.03 + j149.41) - (11 + j143)}{(12.03 + j149.41) + (11 - j143)} = 0.271\angle 65.32^0$$

The relative phase difference between the vertical dipole and the horizontal dipole is 84^0, thus the phase relation requirement is satisfied by the proposed geometry in order to obtain the circular polarization. A modified T-match network is designed to feed the cross dipole structure [166]. The modified T-match feed network with meander line provides more parameters to obtain a complex conjugate impedance matching between the antenna and the tag IC.

3.4 Results and Discussions

The fabricated prototype of the proposed tag antenna with FR4 glass epoxy substrate is presented in figure 3.3. This section discusses about the various results obtained during the analysis of the designed antenna structure. The results that are discussed in the following subsections include input impedance characteristics, reflection coefficient characteristics, axial ratio, radiation patterns and read range. Parametric analysis is also provided to show influence of the length of the semi-circular curve (Lsc) on the input impedance and the CP performance of the proposed cross dipole antenna.

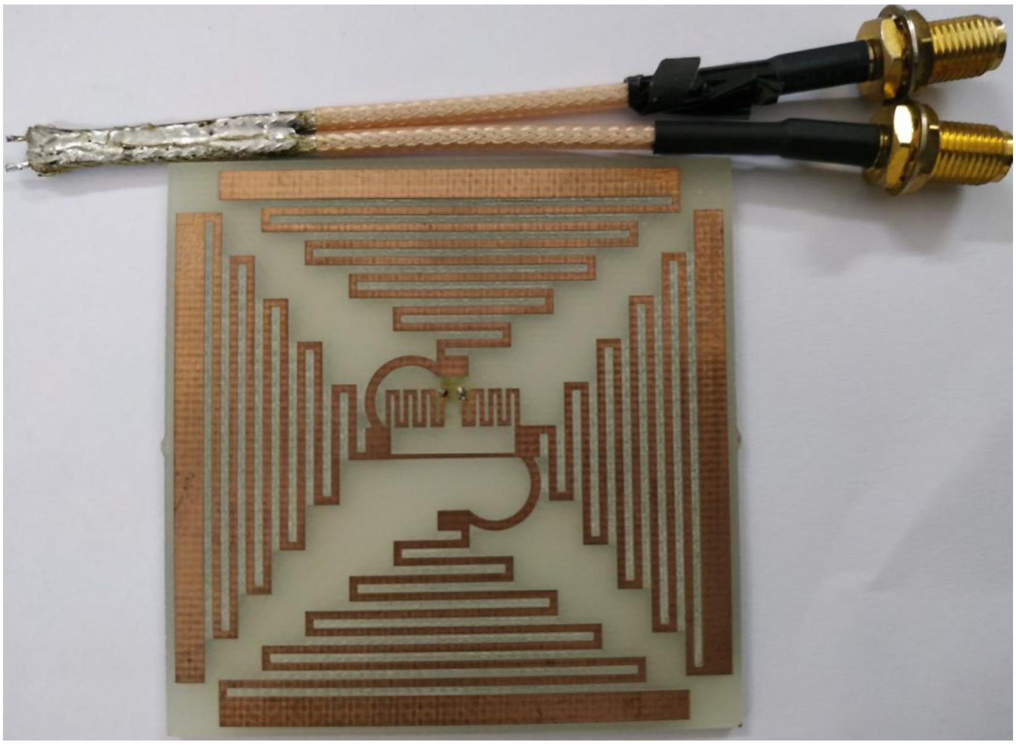

Figure 3.3 Fabricated prototype of the cross dipole CP antenna

3.4.1 Input Impedance versus Frequency Characteristics

The designed cross dipole antenna is a balanced antenna thus its input impedance cannot be measured by using only single ended two-port vector network analyzer. The input impedance of the proposed tag antenna was measured by using a differential probe with Anritsu MS2038C VNA. A differential probe is fabricated by soldering the outer conductor of two semi-rigid coaxial cables. The two small-extended inner conductors at one end of the differential probe are connected to the proposed antenna and the other end of the test fixture is connected to VNA with cables as shown in figure 3.4.

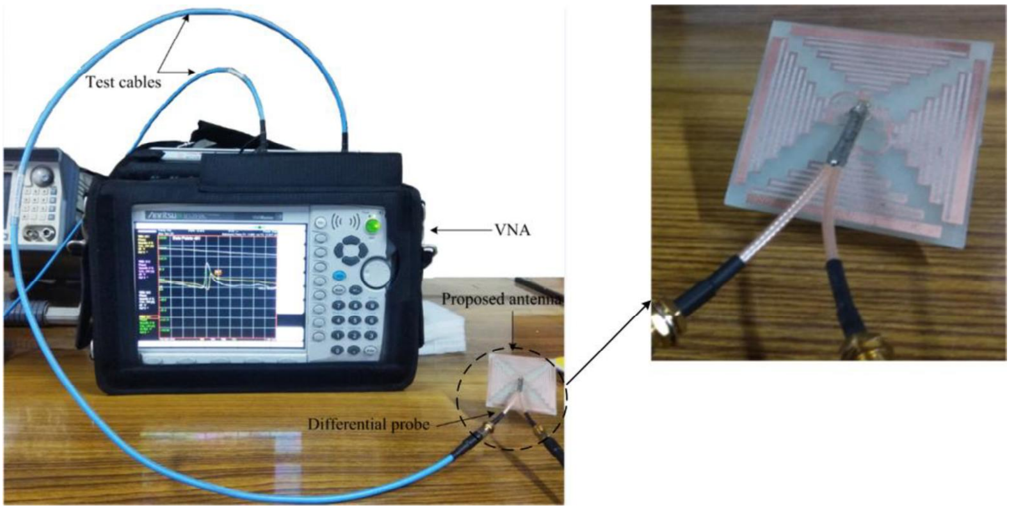

Figure 3.4 Impedance measurement setup of cross dipole CP antenna with VNA

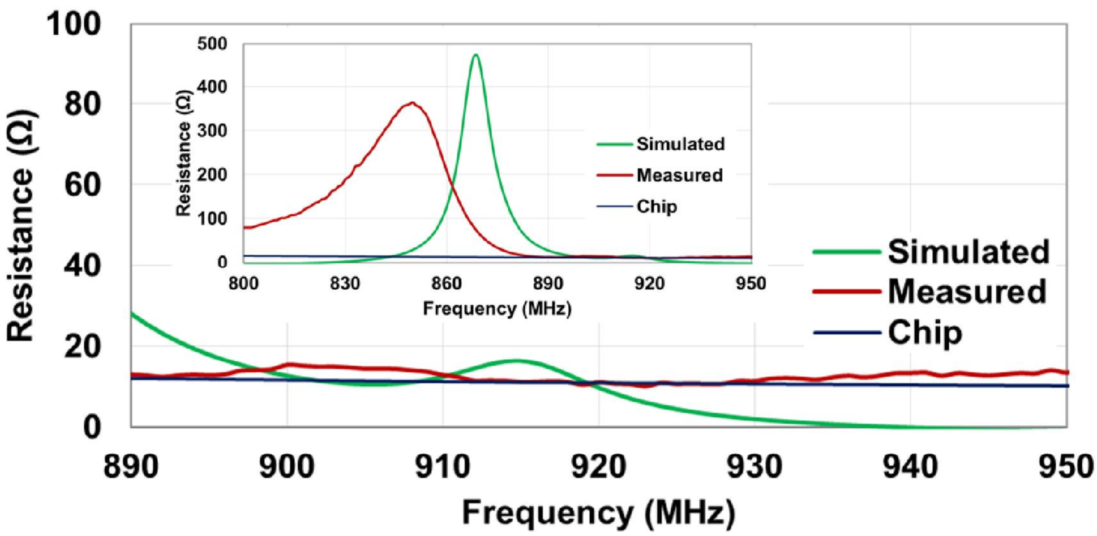

Figure 3.5 Simulated and experimental input resistance of the cross dipole CP antenna

The S-parameters of the proposed antenna are measured and then by using equation (3.1) the differential input impedance (Z_d) of tag antenna is calculated. Figure 3.5 shows the simulated and experimental results of the input resistance of the proposed antenna. Figure 3.6 exhibits the simulated and measured results of the input reactance of the antenna. Simulated input resistance and reactance show good agreement with experimental results around the resonance frequency but at other frequencies there is some discrepancy. Here the impedance is measured indirectly i.e., impedance is calculated by using measured S-parameters. S-parameters are reflection and transmission coefficients. There is deviation in all S-parameters at all frequencies except resonating frequency and in impedance calculation all S-parameters are used so due to the combined effect of mismatching the deviation in the measured results increases in all frequencies except resonating frequency. At 915 MHz, simulated and experimental input impedances of the antenna are 16.34+j142.25 Ω and 11.12+j140.65 Ω, respectively, which are fairly complex conjugate matched with the tag chip input impedance (11-j143 Ω).

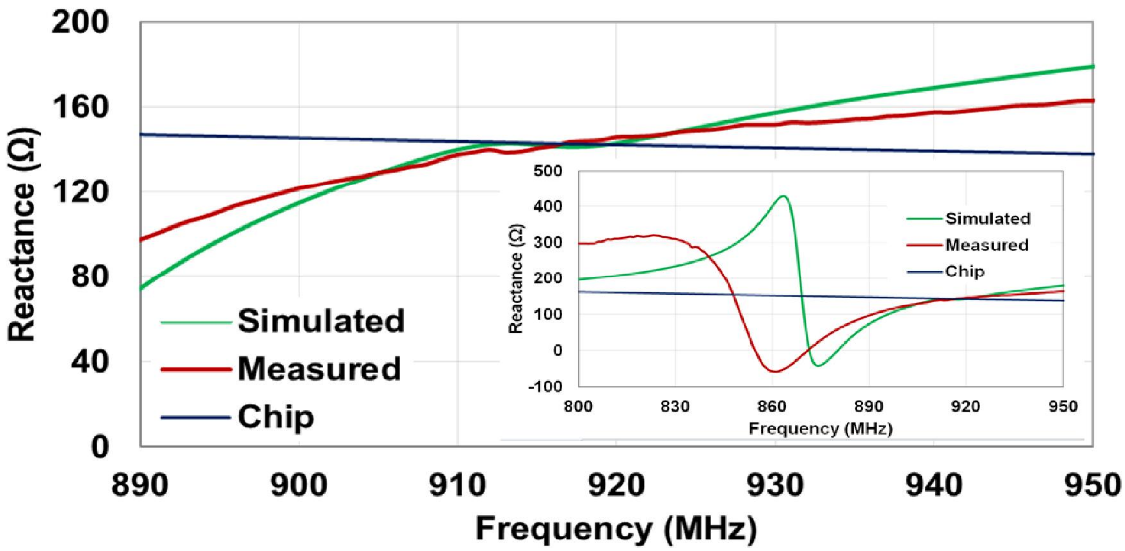

Figure 3.6 Simulated and experimental input reactance of the cross dipole CP antenna

3.4.2 Reflection Coefficient and Axial-ratio Characteristics

The reflection coefficient of the designed antenna is computed from the input impedance results by using equation (3.1). The simulated and measured reflection coefficient and axial ratio are plotted with frequency in figure 3.7. These results illustrate that the simulated and measured 10 dB-return loss bandwidth of the antenna are 16 MHz (909-925 MHz) and 17 MHz (908-923 MHz), respectively. 3 dB axial ratio bandwidth of the antenna is 6 MHz (912-918 MHz), which is within the 10 dB return loss bandwidth.

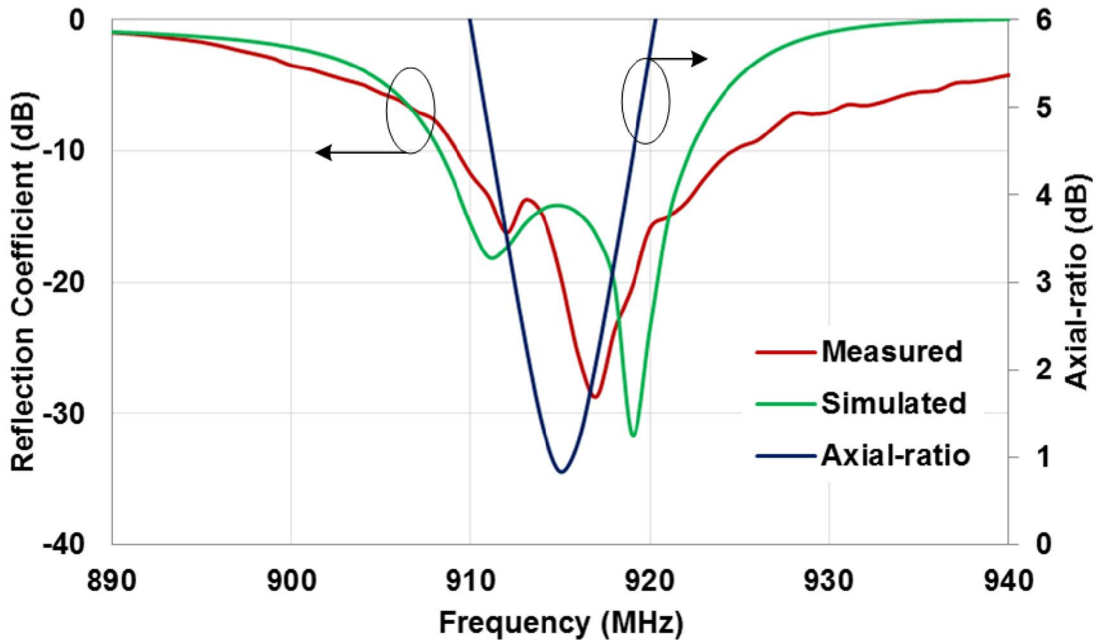

Figure 3.7 Simulated and experimental reflection coefficient of the cross dipole CP antenna and simulated axial ratio

3.4.3 Influence of the Length of Semi-circular Curve

The influence of the length of the semi-circular curve (Lsc) on the input impedance and the CP performance of the proposed cross dipole antenna are exhibited in figures 3.8 – 3.10. Figure 3.8 demonstrates the input impedance of the antenna on tuning the parameter Lsc from 11.3 to 11.7 mm, while keeping all other parameters constant. At the resonating frequency, the input resistance and the input reactance are observed to vary insignificantly, illustrating the independency of the input impedance on the length of semi-circular curve (Lsc). However, a significant impact is noticed on the phase difference between the orthogonal electric field components on varying Lsc. The ratio and the phase difference of the electric fields on the x and y direction with different values of parameter (Lsc) are shown in figure 3.9. As the length Lsc decreases the phase difference between electric field increases and for Lsc=11.5 mm, the phase difference is 88^0 and the ratio between electric fields is 0.3 dB due to which circularly polarized radiation occurs at 915 MHz. The axial ratio of the proposed antenna is demonstrated in figure 3.10 with different values of Lsc. So, by properly tuning the length of semi-circular curve, the CP radiation can be obtained without disturbing the impedance matching with tag IC.

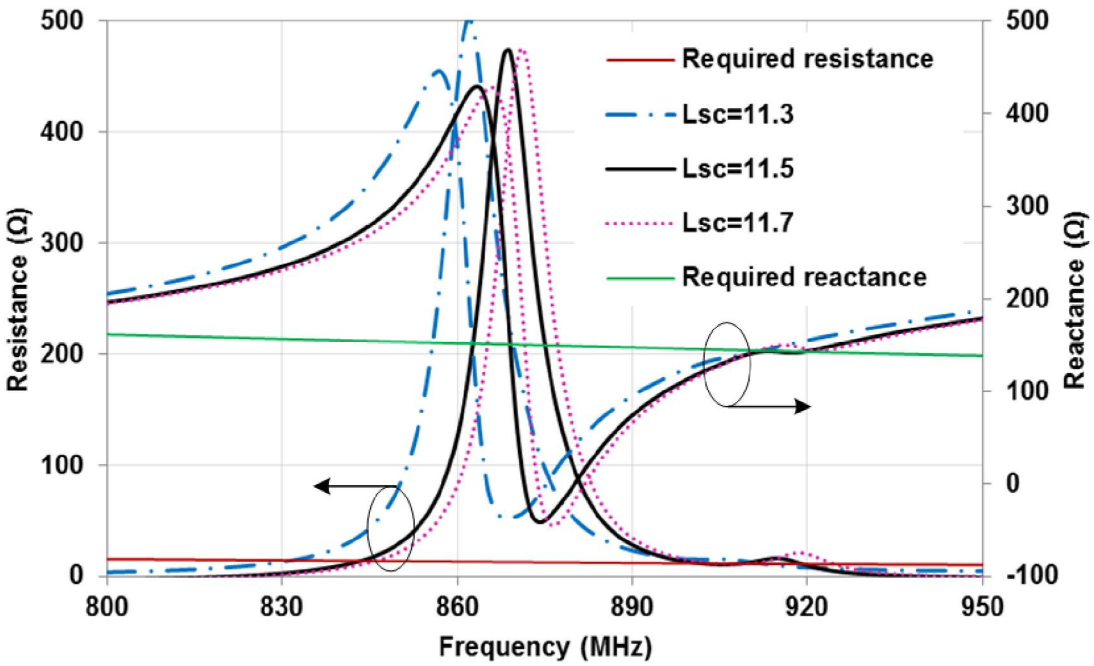

Figure 3.8 Simulated input impedance characteristics of the antenna with variation in length of the semi-circular curve (Lsc)

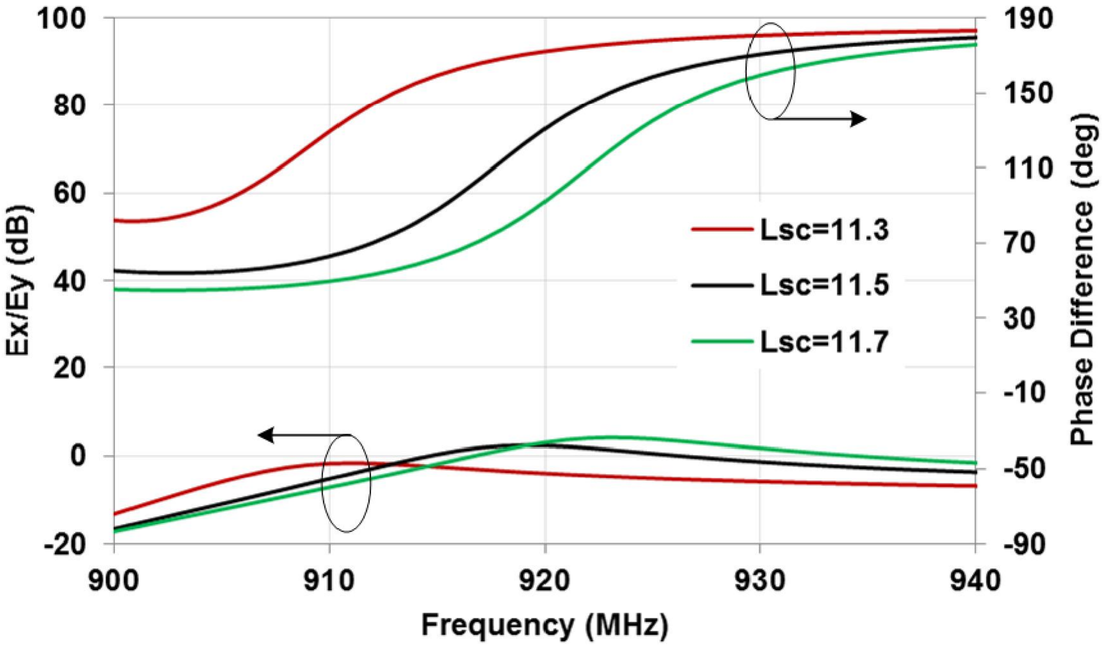

Figure 3.9 Simulated electric field ratio (Ex/Ey) and phase difference characteristics of the antenna with variation in length of the semi-circular curve (Lsc)

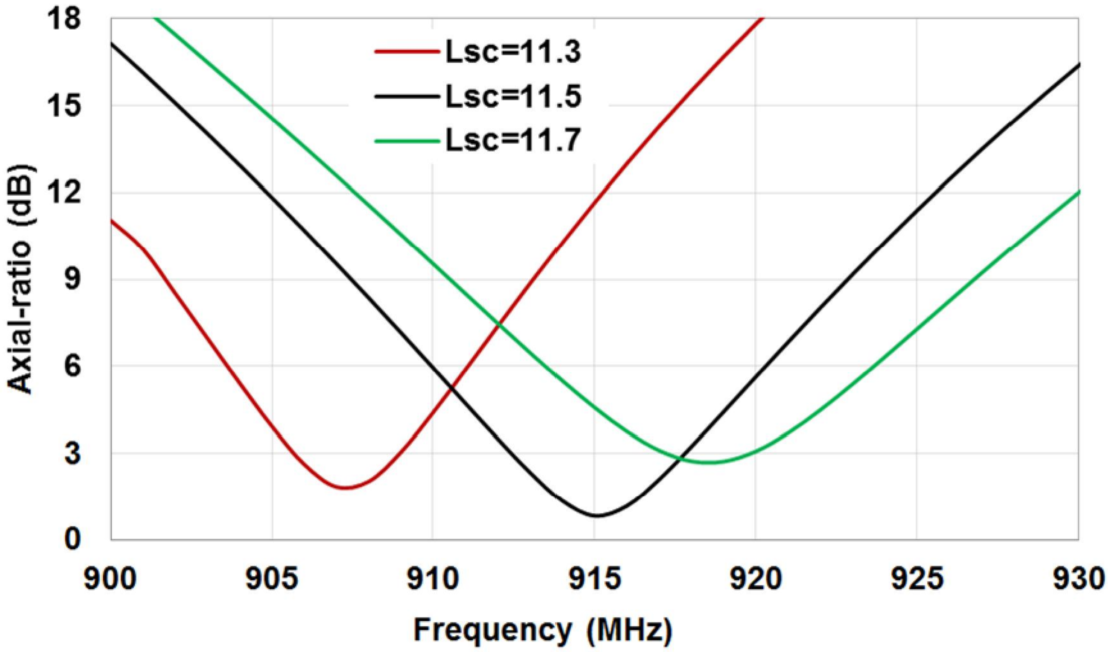

Figure 3.10 Simulated axial ratio characteristics of the antenna with variation in length of the semi-circular curve (Lsc)

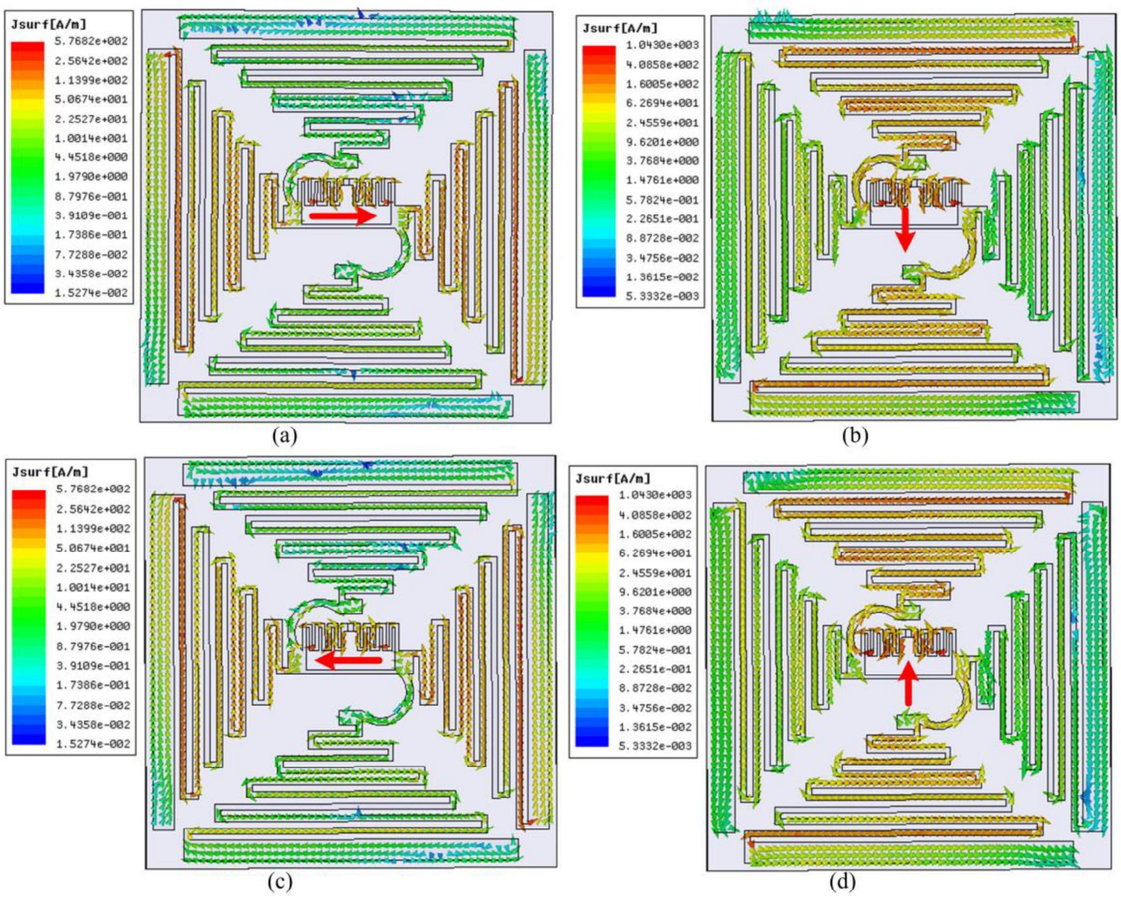

Figure 3.11 Simulated surface current density of the cross dipole CP antenna at 915 MHz at different time phases (a) wt= 0^0, (b) wt=90^0 , (c) wt=180^0, (d) wt=270^0

3.4.4 Surface Current Density Distribution

In order to validate the circularly polarized radiation at 915 MHz, simulated surface current distribution of the proposed antenna is demonstrated at different time phases (wt) 0^0, 90^0, 180^0, and 270^0 as shown in figure 3.11. The surface current of the cross dipole antenna at the boresight rotates in the clockwise direction as wt increases, which generates radiation of left hand circularly polarized wave in boresight direction.

3.4.5 Far Field Radiation Patterns

Input impedance of the designed tag antenna is not matched to 50 Ω, thus conventional anechoic chamber is unable to perform radiation pattern measurement. Therefore, figure 3.12 only demonstrates the simulated radiation pattern of the designed antenna in two principal planes (XZ and YZ planes) at 915 MHz. The cross dipole antenna has a bidirectional radiation pattern. In the boresight direction, it radiates Left Hand Circularly Polarised (LHCP) wave, and in the back side it radiates Right Hand Circularly Polarised (RHCP) wave.

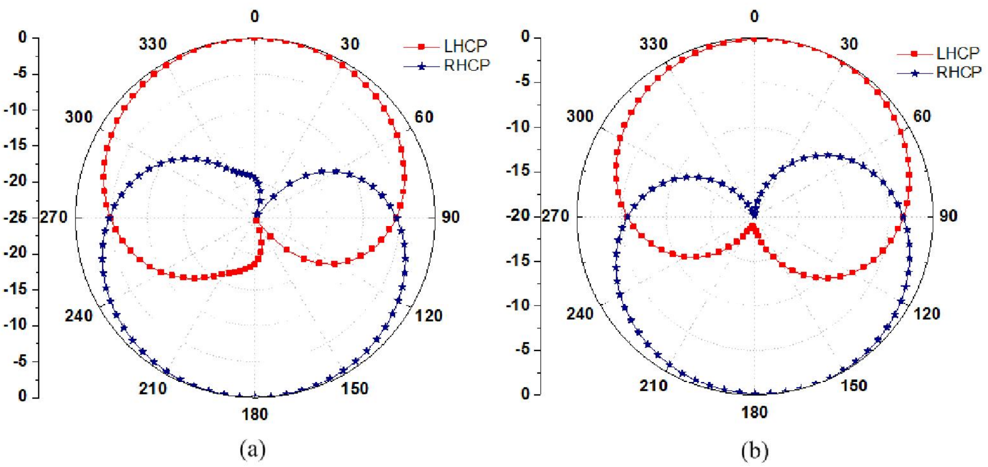

Figure 3.12 Simulated radiation pattern of the cross dipole antenna at 915 MHz (a) XZ plane, and (b) YZ plane

3.4.6 Read Range

The maximum read range of the antenna was calculated by using the Friis transmission equation (2.3). The value of effective isotropic radiated power (product of transmitted power from reader and gain of the reader antenna) used is 4W, which is regulated in accordance with Federal Communications Commission (FCC). The proposed antenna is designed with Impinj Monza-4 tag IC, which requires -17.4 dBm power for activation. The maximum read range of the proposed cross dipole CP antenna is calculated and compared with a linearly polarized dipole antenna. As the proposed circularly polarized antenna is derived from a linearly polarized dipole, a linearly polarized antenna of comparable gain and reflection coefficient is assumed. A comparison of the read range is drawn between the proposed circularly polarized antenna and the assumed structure (linearly polarized antenna) in order to focus on the change in polarization efficiency. Simulated and measured read range are plotted in figure 3.13 and a comparison between the read range of proposed CP antenna and LP dipole antenna is shown in table 3.2.

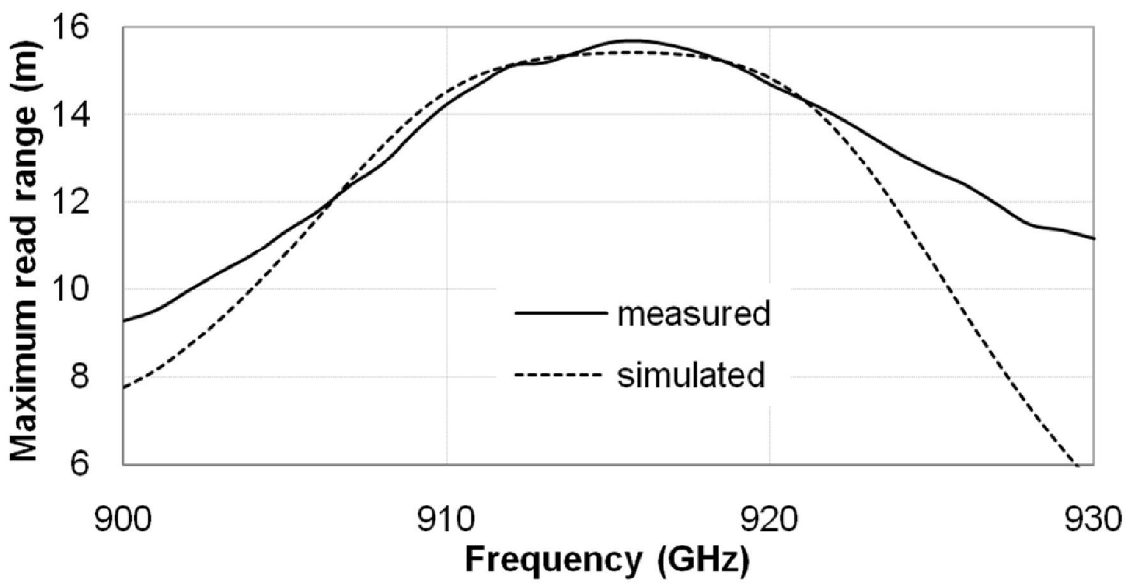

Figure 3.13 Maximum read range of the cross dipole CP antenna

In the case of a linearly polarized dipole antenna, the maximum read range was 10.9 m due to the polarization mismatch (ρ=0.5) between the circularly polarized reader and linearly polarized tag antennas. In case of the proposed CP antenna, there is a good polarization match (ρ=1) between the reader antenna and tag antenna. Therefore, the proposed CP antenna has 4.7 m longer read range than the linearly polarized dipole antenna.

Table 3.2 Comparison between proposed CP antenna and LP antenna in terms of read range

Simulated gain of tag antenna(G_r) at 915 MHz	**Maximum read range (R_{max})**		
	LP dipole (sim.)	**CP proposed antenna (sim.)**	**CP proposed antenna (meas.)**
1.288 dBic	10.9 m	15.42 m	15.66 m

3.5 Comparison with Previously Reported Antennas

Table 3.3 demonstrates comparison among the proposed antenna and previously reported circularly polarized antennas in terms of the maximum read range, antenna size, 3 dB axial ratio bandwidth, gain and threshold activation power.

Table 3.3 Performance comparison of the cross dipole CP antenna with different CP RFID tag antennas

Antenna	**Read range (m)**	**Dimension (mm^2)**	**3 dB AR bandwidth (MHz)**	**Gain at 915 MHz (dBic)**	**Threshold activation power (dBm)**
[135]	10.5	189.6×127.9	-	-	-
[137]	4.3	100×100	20(903-923)	-8.45	-14
[138]	2.2	70×70	6(922-928)	-14.4	-14
[139]	2.5	74×74	6(912-918)	-13.3	-14
[140]	7.2	40×40×π	10(920-930)	0.4	-14
[167]	16.3	90×90	52(895-947)	2.83	-14
Proposed Antenna	15.6	58×58	6(912-918)	1.28	-17.4

The read ranges of the antennas reported in [135], [137]–[140], [167] are computed with circularly polarized readers having EIRP of 4W. The proposed cross dipole antenna has a smaller 3 dB axial ratio bandwidth but size of the antenna is also smaller. The proposed antenna exhibits larger gain and longer reading range except for [167]. However, antenna [167] has larger dimensions compared to the proposed antenna. The read range of the antennas [142] and [166] have been computed with EIRP of 3.28 W, therefore, these antennas are not included in comparison table 3.3. The CP tag antennas in [142], [166] have smaller dimensions, but they have a smaller read range than the proposed antenna.Thus, the comparative study portrays a trade-off between the antenna size and the maximum read range.

3.6 Conclusion

A circularly polarized cross dipole tag antenna for UHF RFID applications has been investigated through simulation and measurement. A linearly tapered meander line with rectangular tip loading at the end has been used in each arm of the cross dipole for size miniaturization of the antenna and at the center, a modified T-match structure has been used in order to get the conjugate impedance matching with tag IC. The measured 10-dB return loss bandwidth and 3-dB axial ratio bandwidth of the proposed cross dipole antenna are 17 MHz (908-923 MHz) and 6 MHz (912-918 MHz), respectively. Furthermore, the maximum read range of the proposed CP antenna is 15.66 m and in case of the linearly polarized dipole antenna of analogous characteristics is 10.9 m. A 4.7 m read range enhancement has been obtained for CP cross dipole antenna to the LP dipole antenna.

The designed cross dipole CP antenna has a single antenna for both receiving and backscattering purpose. Thus, it will not be able to provide sufficient power continuously for the tag chip activation and maximum level difference in the backscattered fields. On the conductive surfaces, only the normal component of the electric field and tangential component of the magnetic field are available. Operation of the designed cross dipole CP antenna depends on the tangential component of electric field thus the performance will be degraded when tagged to metallic objects. Another issue of placing the cross dipole tag on a metallic object is the change of the antenna parameters such as the input impedance, directivity, radiation pattern, and efficiency. Microstrip patch antenna is an obvious solution for metallic object tagging. Microstrip antenna requires a ground plane to operate. Since the ground plane is a part of the antenna design; this type of antenna will not be affected too much when attached to metallic objects. By considering the above facts, a microstrip type dual antenna is designed in the upcoming chapter.